International Journal of Offshore and Coastal Engineering
Vol.9 | No. 2 | pp. 50 – 57 | November 2025
e-ISSN: 2580-0914


Submitted: July 30, 2025 | Revised: September 24, 2025 | Accepted: November 5, 2025

# Analysis The Effect of The Distance Between Concrete Floating Breakwater With Double Configuration On The Mooring Line Force In Catenary System Using Dualsphysics

Noris Yolanda[a], R. Haryo Dwito Armono[b] and Wahyudi[c]

[a)] Department of Ocean Engineering, Institut Teknologi Sepuluh Nopember, Surabaya, Indonesia
[b)] Department of Ocean Engineering, Institut Teknologi Sepuluh Nopember, Surabaya, Indonesia
[c)] Department of Ocean Engineering, Institut Teknologi Sepuluh Nopember, Surabaya, Indonesia
*Corresponding author: norisyolanda727@gmail.com

## ABSTRACT

*Ports are crucial infrastructure supporting a nation's economy. However, port utilization in Indonesia remains suboptimal due to high sea waves that can damage infrastructure and disrupt operations. A solution is the construction of Floating Breakwaters (PGA). This study analyzes the effect of spacing between dual-configured concrete PGAs on mooring rope forces using a catenary system. The Smoothed Particle Hydrodynamics (SPH) method with DualSPHysics software was used to determine maximum stress on the mooring ropes. Results show that PGA spacing influences mooring tension. In variant A, spacing from 20–30 cm reduces the force by 20%, while 30–40 cm increases it by 1%. In variant B, spacing from 50–75 cm increases tension by 8%, while 75 cm–1 m decreases it by 16%. Wave height and period also affect tension. The maximum force for variant A with a single configuration occurs at a wave height of 0.18 m and a period of 2.21 s, reaching around 185 kN at the anchor and 188 kN at the fairlead. For variant B, the maximum is at a height of 0.28 m and a period of 2.84 s, reaching about 360 kN. In dual configuration, maximum force occurs at 0.2 m spacing for variant A and 0.5 m for variant B.*

**Keywords:** *Floating Breakwater, Catenary Mooring System, Mooring Line Tension, Concrete, DualSPHysics..*

## 1. INTRODUCTION

Ports are one of the important infrastructures in supporting the economy in a country. However, the use of ports in Indonesia has not been fully optimal. One of the factors that hinders port optimization is high sea waves. High sea waves can cause damage to port infrastructure, thus disrupting the loading and unloading of goods and passengers. In general, these problems can be solved by building coastal protection structures in the form of breakwaters [1]. However, not all ports in Indonesia can be built with a breakwater using the soil clearing method (*rubblemound breakwater*). Some ports in Indonesia have a deep enough sea depth so that if a breakwater is built, the soil clearing method will take expensive costs and a long time. To overcome these problems, the construction of floating breakwaters (*floating breakwater*) is a solution that must be considered.

Floating breakwaters (PGAs) have brought significant innovations in efforts to protect ports from high sea waves in locations where conventional breakwaters have proven ineffective. Conventional breakwaters require complex planning and construction, and require the use of heavy materials at a low cost. Even so, in deep waters with the same depth, the construction of PGAs has a cheaper cost when compared to conventional breakwaters [2]. Other advantages of PGA are efficiency that is not affected by tides and sea level changes, minimal environmental impact, low construction and demolition costs, short installation times, and the flexibility to adjust modules and layouts to accommodate future changes in use [3].

This study uses the SPH method with DualSPHysics software which has been proven to be accurate in simulating the movement of floating structures under the influence of regular waves [4]. PGA performance is affected by immersion depth and wave conditions, but is hardly affected by the density and gravity of the ballas water [5]. Previous research has shown that twin PGAs are superior in wave filtering over single PGAs [6]. In addition, the distance between PGAs with dual configurations can affect the performance of damping waves and voltages on the mooring rope [7]. This research will model a double-configuration concrete PGA and design a mooring system *catenary* with a variation in distance, focus on the mooring system voltage so as not to exceed the limit *breaking load* appropriate *rules*.

## 2. RESEARCH DESCRYPTION

### 2.1 Research Data

The data needed in this study is the data of the existing *numerical flume tank* model modeled for the simulation. Existing PGAs are also modeled to be simulated on *numerical flume tanks* that have been created for validation aimed at ensuring that the results of numerical experiments reflect real-world situations as accurately as possible. Model data from *numerical flume tanks* and existing PGA can be seen in Table 1.

Table 1. Data Existence

| Data Type | Information | Scaled Value | Unit |
|---|---|---|---|
| PGA Structure Data | Long | 0,745 | m |
| | Wide | 0,5 | m |
| | Tall | 0,3 | m |
| Environmental Data | Depth | 0,514 | m |
| | Wave Height | 0,05 | m |
| | Wave Period | 1,2 | s |

The data that will be used for the simulation in this study is PGA structure data. There are 2 variants of the PGA model that will be compared to the simulation results. The dimensions of each variant will be scaled 1:10 according to the Froude Scale Law shown in Table 2.

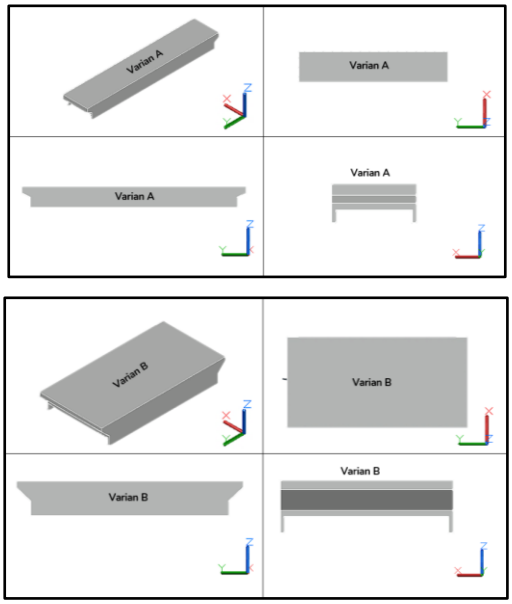


Picture 1. Isometric PGA Variant A and Variant B Appearance

Table 2. PGA Structure Data

| Types of PGAs | Information | Original Value | Scaled Value |
|---|---|---|---|
| Varian A | Long | 20 m | 2 m |
| | Wide | 4 m | 0,4 m |
| | Tall | 1,8 m | 0,18 m |
| | *Freeboard* | 55 ton | 55 kg |
| | Density | 0,5 m | 0,05 m |
| Variant B | Long | 20 m | 2 m |
| | Wide | 10,25 m | 1,025 m |
| | Tall | 3 m | 0,3 m |
| | *Freeboard* | 200 ton | 200 kg |
| | Density | 0,8 m | 0,08 m |

Environmental data parameters are obtained based on real-world conditions, adjusted to the potential location of concrete PGAs. The variation of the environmental data also depends on the PGA variant to be tested. Variant A, designed for calmer ocean conditions, will be tested with environmental data that tends to be smaller than Variant B. The two main parameters to be tested are wave height and wave period which can be seen in Table 3.

Table 3. Environmental Data

| Types of PGAs | Information | Original Value | Scaled Value |
|---|---|---|---|
| Varian A | Wave Height | 1,4 m | 0,14 m |
| | | 1,6 m | 0,16 m |
| | | 1,8 m | 0,18 m |
| | Wave Period | 4 s | 1,26 s |
| | | 6 s | 1,89 s |
| | | 7 s | 2,21 s |
| Variant B | Wave Height | 2 m | 0,2 m |
| | | 2,4 m | 0,24 m |
| | | 2,8 m | 0,28 m |
| | Wave Period | 4 s | 1,26 s |
| | | 7 s | 2,21 s |
| | | 9 s | 2,84 s |

The distance test data between PGA structures is made based on the width of the PGA structure that has been scaled. In accordance with the reference dimensions of the PGA structure contained in Table 3, the distance between the structures will also be adjusted to the scale of 1:10 using the Froude Scale Number. For each variant, the spacing between the structures for the PGA configuration in detail can be seen in Table 4.

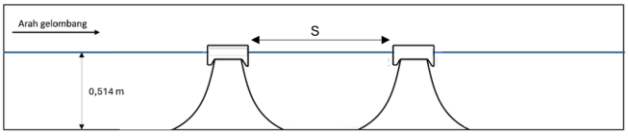


Picture 2. Simulation Scheme

Table 4. Interstructural Test Distance

| Types of PGAs | Distance Variation | Test Distance (m) |
|---|---|---|
| Varian A | 0.5 L | 0,2 |
| | 0.75 L | 0,3 |
| | L | 0,4 |
| Variant B | 0.5 L | 0,5 |
| | 0.75 L | 0,75 |
| | L | 1 |

### 2.2 Numerical Modeling of Flume Tank and PGA Structure

*The numerical data of* the existing tank flume that has been obtained is modeled on DualSPHysics for validation.

The data will be used for further analysis. The schematic of the *numerical flume tank* model is shown by Figure 3.

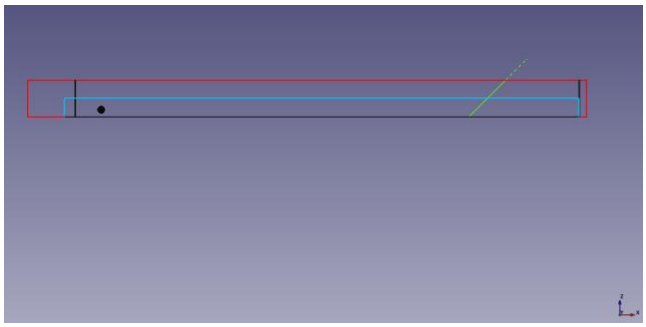

Picture 3. Schematic Model *Numerical Flume Tank* on DualSPHysics

After the numerical flume tank *modeling is carried out*, the modeling validation is carried out to find out that the *tank flume* model that has been made can be used for further analysis. Validation begins with remodeling the existing PGA structure to be simulated on *a previously modeled* tank flume.

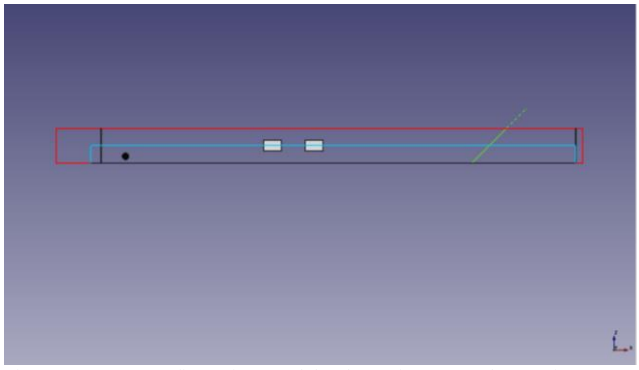

Picture 4. PGA Configuration Model Schematics on DualSPHysics

The simulation results are in the form of PGA or RAO structure movement characteristics compared to the RAO from Chen et al. (2023). The modeling carried out is based on 2D so that the resulting RAO is only *surge*, *heave*, and *pitch*. The tolerance value of the RAO comparison difference must be less than 10%. The validation results shown by Tables 5 – 7 show that the RAO results have a percentage difference of less than 10%. The RAO comparison can also be seen in Figure 4. Therefore, the results of *numerical flume* tank modeling can be used for further analysis.

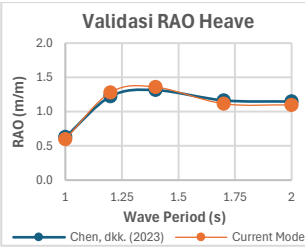


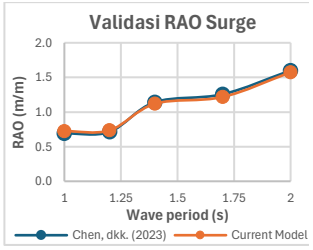


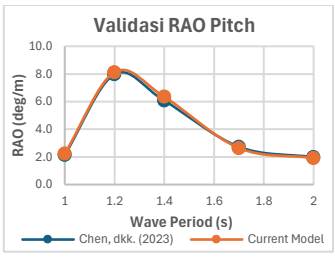


Picture 5. RAO Validation Graph

Table 5. RAO Validation Results *Heave*

| Wave Period (s) | RAO Heave (m/m) | | Error | Remarks |
|---|---|---|---|---|
| | Chen dkk. (2023) | Current Model | | |
| 1 | 0.628 | **0.598** | 4.81% | PASS |
| 1.2 | 1.222 | **1.281** | 4.84% | PASS |
| 1.4 | 1.314 | **1.358** | 3.34% | PASS |
| 1.7 | 1.164 | **1.115** | 4.23% | PASS |
| 2 | 1.147 | **1.098** | 4.27% | PASS |

Table 6. RAO Validation Results *Surge*

| Wave Period (s) | RAO Surge (m/m) | | Error | Remarks |
|---|---|---|---|---|
| | Chen dkk. (2023) | Current Model | | |
| 1 | 0.691 | **0.724** | 4.71% | PASS |
| 1.2 | 0.714 | **0.736** | 3.04% | PASS |
| 1.4 | 1.143 | **1.12** | 2.00% | PASS |
| 1.7 | 1.257 | **1.218** | 3.11% | PASS |
| 2 | 1.6 | **1.574** | 1.63% | PASS |

Table 7. RAO Validation Results *Pitch*

| Wave Period (s) | RAO Pitch (deg/m) | | Error | Remarks |
|---|---|---|---|---|
| | Chen dkk. (2023) | Current Model | | |
| 1 | 2.148 | **2.236** | 4.11% | PASS |
| 1.2 | 7.977 | **8.122** | 1.81% | PASS |
| 1.4 | 6.068 | **6.347** | 4.59% | PASS |
| 1.7 | 2.727 | **2.641** | 3.16% | PASS |
| 2 | 1.977 | **1.921** | 2.85% | PASS |

### 2.3 Structural Modeling of Variant A and Variant B

The PGA Variant A and B models were modeled using FreeCAD software and then integrated with the *numerical flume tank model* that had previously been validated. This PGA model follows the model data that has previously been obtained from the dimensions, structure, and geometry of the PGA that have been scaled as shown in Table 2. The results of modeling the structure of PGA can be seen in Figure 5 and Figure 6.

Picture 6. PGA Variant A Modeling Scheme on DualSPHysics

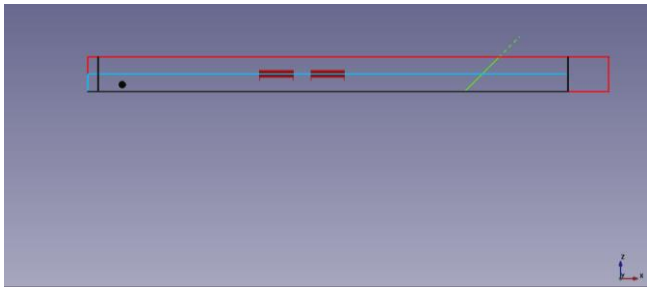

Picture 7. PGA Variant B Modeling Scheme on DualSPHysics

### 2.4 Mooring System Modeling

Modeling of mooring ropes on PGA was carried out using DualSPHysics software. The modeling of the mooring system configuration was carried out with a configuration of 2 *symmetrical mooring lines*. The specifications of the mooring rope used in this study are shown in Table 8.

Table 8 Specification of Mooring Rope

| Description | Scaled Value |
|---|---|
| Rope Length | 1,2 m |
| Diameter | 3,6 mm |
| Mass per unit length | 66 kg/100 m |
| *Stiffness* | 2900 N |
| MBL | 1020.2 N |
| Material | High Modulus Polyethylene 'Dynema ® SK75' |

The configuration of the mooring rope on the PGA is symmetrical on each side. To make the analysis process easier, each rope has been given a name to define it. The naming of the mooring rope in detail is shown by Figure 8.

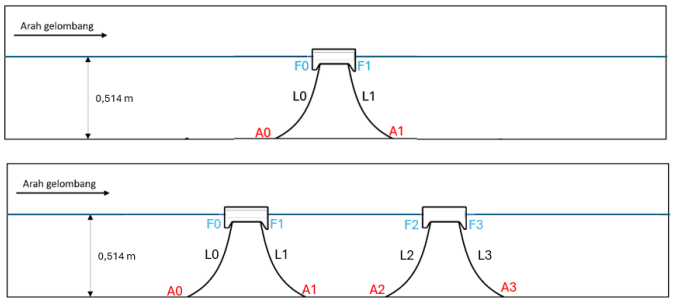


Picture 8. Single and Dual Configuration PGA Mooring Rope Naming

## 3. RESULTS AND DISCUSSION

### 3.1 Influence of Hydrodynamic Parameters

The Tension that occurs on the mooring rope is affected by the hydrodynamic parameters, i.e. the wave period and wave height. The variation in hydrodynamic parameters shows different stress values. Regardless of the variant used, hydrodynamic parameters show an influence on the maximum stress value that occurs in PGA. To measure the influence of hydrodynamic parameters, it can be seen through the change in the non-dimensional magnitude of the wave slope on the mooring rope force. . $\left({}^{H}/_{gT^2}\right)$

Figure 9 shows the relationship between wave slope and mooring rope force in PGA variant A. The results show that the trend of mooring rope force tends to decrease along with the increase in wave slope. However, when viewed in more detail, it can be seen that the mooring rope force has a similar pattern in terms of the increase in rope force that occurs. The pattern of increasing the maximum tension value of the mooring rope can be observed at each variation in wave height and a given wave period. This suggests that although in general the mooring rope force decreases with increasing wave slope, there are specific moments where the maximum tension experiences a consistent increase, reflecting the complexity of the interaction between the wave and the mooring rope.

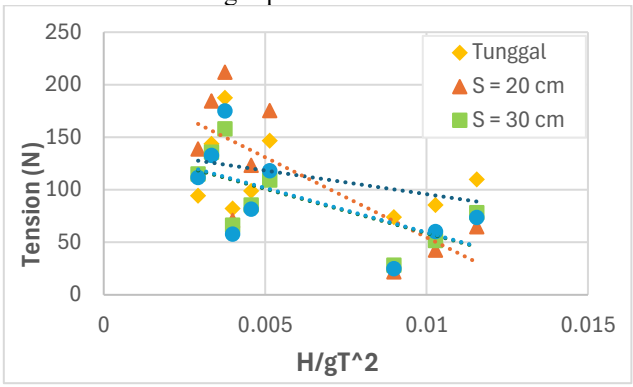


Picture 9. Relationship of Wave Slope to Mooring Rope (Variant A)

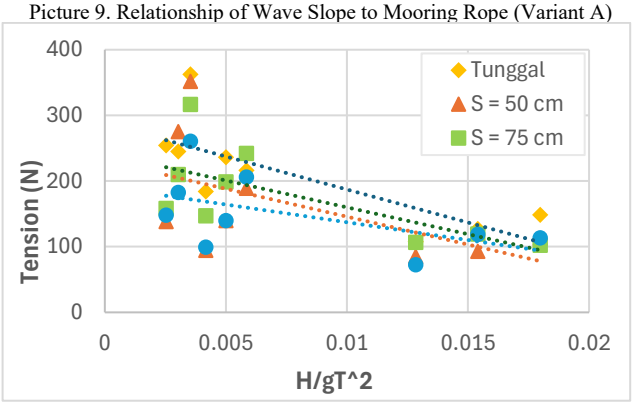


Figure 10. Relationship of Wave Slope to Mooring Rope (Variant B)

PGA variant B has the same pattern as variant A, namely the trend of the mooring rope style which tends to decrease with the slope of the wave as shown in Figure 10**.** However,

there is still a pattern of increasing the maximum tension value of the mooring rope at each wave height and a certain wave period. This shows that the slope of the wave has an influence on the tension of the mooring rope. Thus, hydrodynamic parameters can affect the magnitude of the mooring rope force that occurs in PGA for both variants.

### 3.2 Dual Configuration Mooring Rope Tension Analysis

In addition to the parameters of wave height and wave period, another parameter that will be discussed in this study is the distance between the structures which is devoted to analyzing the effect of the distance between PGA structures in a dual configuration on the mooring rope force. The comparison of the distance between the PGA structure and the mooring rope force is shown by Figure 11 and Figure 12. Both variants provide results in the form of a trend in the style of mooring ropes that tend to be inconsistent with the distance between structures.

PGA Variant A has the same pattern at T = 1.89 s and T = 2.21 s for each Hs condition, which has a decrease in the mooring rope force from a distance of 20 cm to a distance of 30 cm by 6 – 38%. Then, from a distance of 30 cm to 40 cm, the force of the mooring rope also decreased by 2 – 13%, except for Hs = 1.8 m which increased by 8 – 11%. Meanwhile, for T = 1.26 s has a different trend compared to other T variations. At a distance of 20 cm to 30 cm, the force of the mooring rope tends to increase by 21 – 30% and decreases at a distance of 30 cm to 40 cm by 6 – 12%.

PGA Variant B shows a different trend from Variant A. At T = 1.26 s, the mooring rope force increases by 25 – 28% from a distance of 50 cm to 75 cm, and from a distance of 75 cm to 1 m decreases by 32%. There was an anomaly that occurred in the period T = 1.26 s, namely when the wave height was 2.8 m, where the mooring rope force decreased by 10% from a distance of 50 cm to 75 cm and an increase of 11% from a distance of 75 cm to 1 m. When T = 2.21 s, the mooring rope force showed a similar trend, namely an increase from a distance of 50 cm to 75 cm by 28 – 56% and a decrease from a distance of 75 cm to 1 m by 15 – 32%.

Overall, the difference in distance has a significant influence on the magnitude of the mooring rope force. In variant A, the average decrease in mooring rope force is 20% from a distance of 20 cm to 30 cm and an increase of 1% from a distance of 30 cm to 40 cm. Meanwhile, in variant B, the average increase in mooring rope force is 8% and a decrease of 16% from a distance of 75 cm to 1 m. However, the large number of anomalies that occur suggests that more research is needed to better understand this phenomenon and reduce the uncertainty that exists in the results obtained. This is important to ensure that the analysis carried out truly reflects real conditions and can be used as a basis for more accurate decision-making in the future.

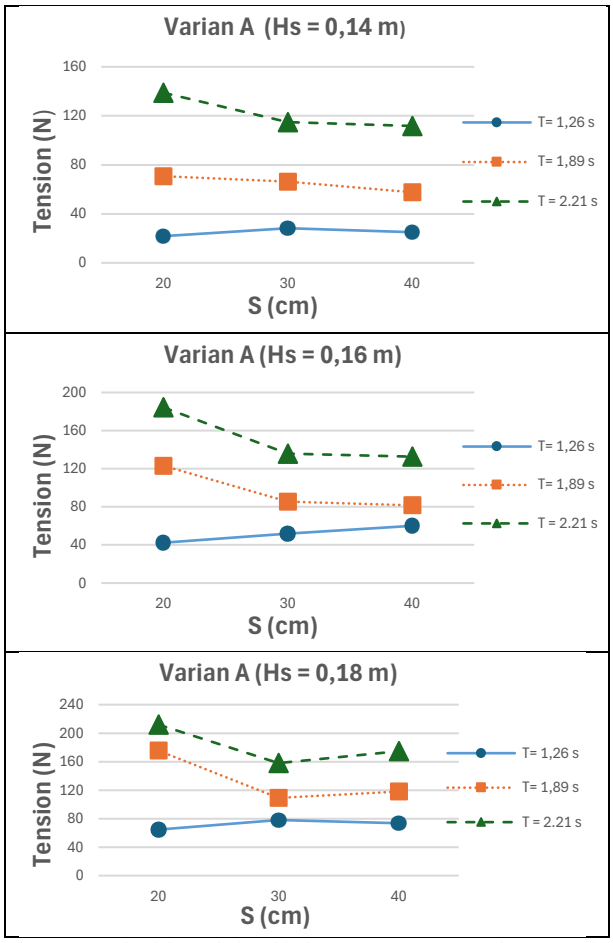


Figure 11. Graph of the Relationship between Structures to the Force of the Mooring Rope (Variant A)

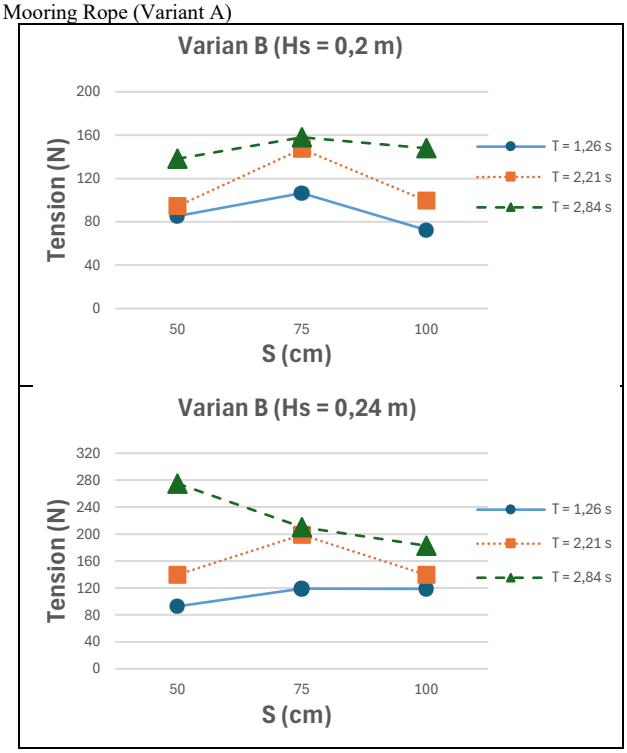

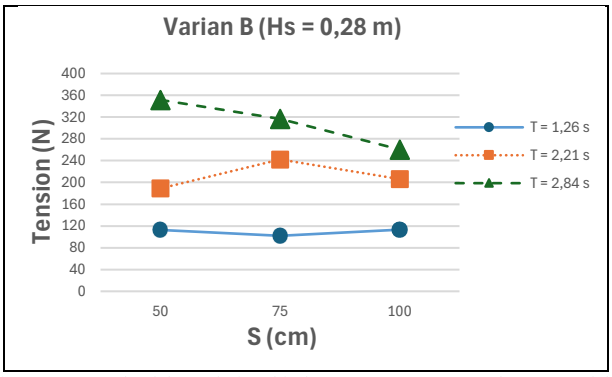


Figure 12. Graph of the Relationship between Structures to the Force of the Mooring Rope (Variant B)

### 3.3 Comparison of Single and Dual Configurations

The comparison of mooring rope styles between single and double configurations for both variants is shown by Table 9. and **Error! Reference source not found.**Table 10.

Table 9. Comparison of PGA Variant A Single and Dual Configuration

| Configuration Type | Average Maximum Voltage (N) | Maximum Voltage Value Drop compared to Single Configuration |
|---|---|---|
| Single | **113.54** | - |
| Ganda S = 20 cm | **114.80** | **1.11%** |
| Ganda S = 30 cm | **91.95** | **-19.01%** |
| Ganda S = 40 cm | **92.80** | **-18.27%** |

Table 10. Comparison of PGA Variant B Single and Dual Configurations

| Configuration Type | Average Maximum Voltage (N) | Maximum Voltage Value Drop compared to Single Configuration |
|---|---|---|
| Single | **209.05** | - |
| Ganda S = 50 cm | **164.28** | **-21.42%** |
| Ganda S = 75 cm | **177.79** | **-14.95%** |
| Ganda S = 100 cm | **148.99** | **-28.73%** |

It can be seen in Table 9 that dual configurations almost always have the ability to reduce mooring rope tension compared to single configurations. The distance configuration that has the best ability to reduce the tension of the mooring rope is 30 cm, with a reduction of 19.01%. However, in the configuration of the distance between the structures of 20 cm, there is an increase in the mooring rope force by 1%. Although this number is still relatively small, this increase indicates the variability in the response of the mooring rope to changes in the distance between structures. Overall, the average reduction in mooring rope force by the dual configuration of variant A is 12.06% compared to the single configuration.

The result of the dual configuration of variant B has always had the ability to reduce the mooring rope force compared to the single configuration as shown by Table 10. The best distance configuration that has the ability to reduce the tension of the mooring rope is 100 cm with a reduction of 28.73%. The average reduction in mooring rope force by the dual configuration of variant B was 21.7% compared to the single configuration.

### 3.4 Safety Factor Testing

In the rope tension analysis of PGA Variant A and B structures, the results of the maximum tension are used to calculate the *safety factor* in all loading conditions. According to the API, the safety factor of the mooring rope configuration during dynamic conditions is 1.67. The results of the calculation of the safety factor are shown in Tables 11 – 14. Based on the results of the maximum tension of the mooring rope, its safety factor is valued above 1.67 which means the configuration of the mooring system and its properties are fit to operate.

Table 11 *Safety Factor* Single Variant A Mooring Rope Tension

| Wave Height (m) | Wave Period (s) | Max Tension (N) | MBL(N) | Safety Factor | Status |
|---|---|---|---|---|---|
| 0.14 | 1.26 | 73.990 | 1020.2 | 13.79 | PASS |
| | 1.89 | 82.075 | | 12.43 | PASS |
| | 2.21 | 94.191 | | 10.83 | PASS |
| 0.16 | 1.26 | 85.404 | | 11.95 | PASS |
| | 1.89 | 98.747 | | 10.33 | PASS |
| | 2.21 | 143.531 | | 7.11 | PASS |
| 0.18 | 1.26 | 109.832 | | 9.29 | PASS |
| | 1.89 | 146.574 | | 6.96 | PASS |
| | 2.21 | 187.540 | | 5.44 | PASS |

Table 12 *Safety Factor* Single Variant B Mooring Rope Tension

| Wave Height (m) | Wave Period (s) | Max Tension (N) | MBL(N) | Safety Factor | Status |
|---|---|---|---|---|---|
| 0.2 | 1.26 | 107.50 | 1020.2 | 9.49 | PASS |
| | 2.21 | 184.10 | | 5.54 | PASS |
| | 2.84 | 254.41 | | 4.01 | PASS |
| 0.24 | 1.26 | 126.94 | | 8.04 | PASS |
| | 2.21 | 236.25 | | 4.32 | PASS |
| | 2.84 | 245.12 | | 4.16 | PASS |
| 0.28 | 1.26 | 148.36 | | 6.88 | PASS |
| | 2.21 | 216.40 | | 4.71 | PASS |
| | 2.84 | 362.42 | | 2.81 | PASS |

Table 13 *Safety Factor* Tension Mooring Rope Variant A Dual Configuration

| No. | Description | Wave Period (s) | Max. Tension (N) | MBL(N) | Safety Factor | Status |
|---|---|---|---|---|---|---|
| **A.** | **Hs = 0.14 m** | | | | | |
| 1 | S = 0.2 m | 1.26 | 35.95 | 1020.2 | 28.38 | PASS |
| | | 1.89 | 70.75 | | 14.42 | PASS |
| | | 2.21 | 138.82 | | 7.35 | PASS |
| 2 | S= 0,3 m | 1.26 | 44.33 | | 23.01 | PASS |
| | | 1.89 | 66.33 | | 15.38 | PASS |

| No. | Description | Wave Period (s) | Max. Tension (N) | MBL(N) | Safety Factor | Status |
|---|---|---|---|---|---|---|
| | | 2.21 | 114.94 | | 8.88 | PASS |
| 3 | S=0,4 m | 1.26 | 40.41 | | 25.25 | PASS |
| | | 1.89 | 57.64 | 1020.2 | 17.70 | PASS |
| | | 2.21 | 111.73 | | 9.13 | PASS |
| **B.** | **Hs = 0.16 m** | | | | | |
| 1 | S = 0.2 m | 1.26 | 48.54 | | 21.02 | PASS |
| | | 1.89 | 123.10 | 1020.2 | 8.29 | PASS |
| | | 2.21 | 184.36 | | 5.53 | PASS |
| 2 | S= 0,3 m | 1.26 | 61.32 | | 16.64 | PASS |
| | | 1.89 | 85.31 | 1020.2 | 11.96 | PASS |
| | | 2.21 | 135.83 | | 7.51 | PASS |
| 3 | S= 0,4 m | 1.26 | 60.04 | | 16.99 | PASS |
| | | 1.89 | 81.60 | 1020.2 | 12.50 | PASS |
| | | 2.21 | 132.67 | | 7.69 | PASS |
| **C.** | **Hs = 0.18 m** | | | | | |
| 1 | S = 0.2 m | 1.26 | 61.27 | | 16.65 | PASS |
| | | 1.89 | 175.43 | 1020.2 | 5.82 | PASS |
| | | 2.21 | 211.93 | | 4.81 | PASS |
| 2 | S= 0,3 m | 1.26 | 78.08 | | 13.07 | PASS |
| | | 1.89 | 109.12 | 1020.2 | 9.35 | PASS |
| | | 2.21 | 157.98 | | 6.46 | PASS |
| 3 | S= 0,4 m | 1.26 | 73.68 | | 13.85 | PASS |
| | | 1.89 | 118.02 | 1020.2 | 8.64 | PASS |
| | | 2.21 | 174.86 | | 5.83 | PASS |

Table 14 *Safety Factor* Tension Mooring Rope Variant B Dual Configuration

| No. | Description | Wave Period (s) | Max. Tension (N) | MBL(N) | Safety Factor | Status |
|---|---|---|---|---|---|---|
| **A.** | **Hs = 0.2 m** | | | | | |
| | | 1.26 | 94.46 | | 10.80 | PASS |
| 1 | S = 0.5 m | 2.21 | 85.32 | 1020.2 | 11.96 | PASS |
| | | 2.84 | 131.44 | | 7.76 | PASS |
| | | 1.26 | 106.51 | | 9.58 | PASS |
| 2 | S= 0.75m | 2.21 | 147.20 | 1020.2 | 6.93 | PASS |
| | | 2.84 | 158.00 | | 6.46 | PASS |
| | | 1.26 | 99.46 | | 10.26 | PASS |
| 3 | S= 1 m | 2.21 | 72.47 | 1020.2 | 14.08 | PASS |
| | | 2.84 | 147.99 | | 6.89 | PASS |
| **B.** | **Hs = 0.24 m** | | | | | |
| | | 1.26 | 139.56 | | 7.31 | PASS |
| 1 | S = 0.5 m | 2.21 | 92.69 | 1020.2 | 11.01 | PASS |
| | | 2.84 | 275.01 | | 3.71 | PASS |
| | | 1.26 | 118.99 | | 8.57 | PASS |
| 2 | S= 0.75 m | 2.21 | 198.80 | 1020.2 | 5.13 | PASS |
| | | 2.84 | 210.08 | | 4.86 | PASS |
| 3 | S= 1m | 1.26 | 118.75 | 1020.2 | 8.59 | PASS |
| | | 2.21 | 139.64 | | 7.31 | PASS |
| | | 2.84 | 182.70 | | 5.58 | PASS |
| **C.** | **Hs = 0.28 m** | | | | | |
| | | 1.26 | 112.90 | | 9.04 | PASS |
| 1 | S = 0.5 m | 2.21 | 188.90 | 1020.2 | 5.40 | PASS |
| | | 2.84 | 323.27 | | 3.16 | PASS |
| | | 1.26 | 101.98 | | 10.00 | PASS |
| 2 | S= 0.75 m | 2.21 | 242.12 | 1020.2 | 4.21 | PASS |
| | | 2.84 | 315.63 | | 3.23 | PASS |
| | | 1.26 | 113.24 | | 9.01 | PASS |
| 3 | S= 1 m | 2.21 | 206.10 | 1020.2 | 4.95 | PASS |
| | | 2.84 | 256.24 | | 3.98 | PASS |

## 4. CONCLUSION/SUMMARY

Based on the analysis of the influence of the distance of the concrete floating breakwater with multiple configurations on the mooring rope force, the distance between the PGA structures significantly affects the magnitude of the mooring rope force. In variant A, the mooring rope force decreases by 20% from a distance of 20 cm to 30 cm and increases by 1% from a distance of 30 cm to 40 cm. In variant B, the mooring rope force increased by 8% and decreased by 16% from a distance of 75 cm to 1 m, with a number of anomalies indicating the need for further research. Wave height and duration also affect the mooring rope style on both PGA variants, with significant changes between single and double configurations despite similar trends. The maximum tension on the mooring rope varies: the single-configuration A variant reaches 185.189 kN at anchor and 187.54 kN at fairlead at 0.18 meters wave height and 2.21 sec wave period; The single configuration B variant reaches 359.75 kN at anchor and 362.42 kN at fairlead at a wave height of 0.28 meters and a wave period of 2.84 seconds. In the dual configuration, variant A reaches 221.93 kN on the L2 mooring line on the fairlead with a distance of 0.2 m, a wave height of 0.18 m, and a wave period of 2.21 s; variant B reaches 323.27 N on the mooring line L0 and L2 on the fairlead with a distance of 0.5 m, wave height of 0.28 m, and a wave period of 2.84 s. The average reduction in mooring rope force by dual configuration was 12.06% for variant A and 21.7% for variant B. The safety factor for all variations was above 1.67, indicating that the configuration of the mooring system and its properties were fit for operation.

## 5. ACKNOWLEDGMENTS

The author would like to express his gratitude to Allah SWT. Not to forget, I would like to thank the Department of Marine Engineering for facilitating me in working on this research. Hopefully the hard work and dedication of all of us will bring great benefits to the development of science.

## REFERENCES

[1] I. A. Hakiki and L. E. Sembiring, "Hydraulic Model Test of Performance of Concrete Floating Breakwater with Dual Configuration," *J. Tek. Hydraul.*, vol. 11, no. 2, pp. 83–92, Dec. 2020, doi: 10.32679/jth.v11i2.629.

[2] T. Habibi, "ANALYSIS OF MOTION BEHAVIOR AND MOORING ROPE FORCE OF LINK SYSTEM ON POROUS SAW-TYPE FLOATING BREAKWATER," SEPULUH NOPEMBER INSTITUTE OF TECHNOLOGY, SURABAYA, 2020.

[3] P. Ruol, L. Martinelli, and P. Pezzuto, "Experimental and NumericalInvestigation of the Effect of Mooring Stiffness on the Behaviour of π-TypeFloating Breakwaters," International Society of Offshore and Polar Engineers, 2012.

[4] J. M. Domínguez *et al.*, "SPH simulation of floating structures with moorings," *Coast. Eng.*, vol. 153, Nov. 2019, doi: 10.1016/j.coastaleng.2019.103560.

[5] Z. Liu and Y. Wang, "Numerical studies of submerged moored box-type floating breakwaters with different shapes of cross-sections using SPH," *Coast. Eng.*, vol. 158, Jun. 2020, doi:10.1016/j.coastaleng.2020.103687.

[6] Y. kun Chen, Y. Liu, D. D. Meringolo, and J. ming Hu, "Study on the hydrodynamics of a twin floating breakwater by using SPH method," *Coast. Eng.*, vol. 179, Jan. 2023, doi: 10.1016/j.coastaleng.2022.104230.

[7] C. Ji, X. Deng, and Y. Cheng, "An experimental study of double-row floating breakwaters," *J. Mar. Sci. Technol.*, vol. 24, no. 2, pp. 359–371, Jun. 2019, doi: 10.1007/s00773-018-0554-2.